View Article Online / Journal Homepage / Table of Contents for this issue
Dynamic Article Links

RSC Advances

Cite this: *RSC Advances*, 2012, **2**, 9899–9903

www.rsc.org/advances

PAPER

Temperature dependent phonon Raman scattering of Heusler alloy $Co_2Mn_xFe_{1-x}Al$/GaAs films grown by molecular-beam epitaxy

Zhenni Zhan,[a] Zhigao Hu,*[a] Kangkang Meng,[b] Jianhua Zhao[b] and Junhao Chu[a]

Received 21st June 2012, Accepted 16th August 2012
DOI: 10.1039/c2ra21255b

Published on 16 August 2012. Downloaded on 25/12/2014 07:15:28.

$Co_2Mn_xFe_{1-x}Al$ full-Heusler alloy films have been grown on GaAs (001) by molecular-beam epitaxy. Three representative phonon modes observed from Raman scattering show different variation trends in the temperature range 87–873 K. The $2F_{1u}$ modes at 569 and 947 cm^{-1} show anomalous change with increasing temperature, which can be due to the phase transition. The Curie temperature (T_c) can be evaluated as 828 K for $x = 0$, 823 K for $x = 0.3$, 818 K for $x = 0.7$, and 788 K for $x = 1$, respectively. This can be ascribed to the fact that the lattice parameter of the films becomes larger with Mn composition.

1 Introduction

Full-Heusler alloys, a relatively promising kind of ferromagnetic material, have been intensively investigated since de Groot first predicted that the Heusler alloys of NiMnSb and PtMnSb exhibit half metallic behavior. These ferromagnets possess a gap at the Fermi level in one of the spin-up and spin-down states, but exhibit metallic behavior in the others.[1,2] They are now being considered as potential materials for applications in the field of spin-electronic and magneto resistive devices. On the applicable viewpoints, it is required that the ferromagnetic materials used as an electrode of magnetic tunnel junctions (MTJs) for tunneling magnetoresistance (TMR) have a high Curie temperature (T_c) as well as a high spin polarization.[3] This qualification can make the devices work well at room temperature. Actual Heusler alloys belong to a group of ternary intermetallics with the stoichiometric composition X_2YZ, where X and Y are transition metal atoms and Z is usually an sp-element, respectively. Among all full-Heusler alloys, Co_2-based compounds are of particular interest, since they have a comparatively high T_c.[4,5] It opens up a promising path to design and realize the spin-electronic devices. Recently, some theoretical investigations have been done to analyze the T_c and its intrinsic physical mechanism. For example, Umetsu *et al.* have reported a T_c of Co_2MnAl with both the $B2$ and $L2_1$ phases by temperature-dependent thermomagnetization curves.[6] Thoene *et al.* calculated the T_c values for a variety of Heusler compounds by mean-field approximation (MFA).[7] The Curie points of Co_2 TiGa and Co_2 FeGa have been evaluated by the first-principles density functional theory combined with a linear response method.[8] However, the crucial issue is still under debate because the experimental results from the material growth and characterizations are scarce.

As we know, the parameter T_c is in connection with the crystalline structure. Correspondingly, the lattice vibrations and/or phonon modes, which can be perturbed by temperature, pressure, and doping, are directly related to the change of structure. Raman spectroscopy is a nondestructive and sensitive technique for investigating structure modification, which can give information on the variations of lattice vibrations.[9,10] Thus, it is a powerful tool for the study of phase transformation and structure evolution. One can apparently evaluate the T_c values by investigating the evolution of phonon modes with temperature. There have been several theoretical works on the phonon modes of Heusler compounds in the past decades.[11,12] However, no experimental evidence has been reported to confirm the T_c of Co-based Heusler alloys by Raman spectroscopy, regardless of the fact that the parameter is very important for spin-electronic device applications. As compared to other techniques, such as magnetic moment measurements, Raman scattering takes advantage of the direct observations of the structure and compatible experimental configuration, especially for the evaluated temperature range.[9]

In this paper, we present temperature-dependent ultraviolet Raman experiments to judge the critical T_c values of epitaxial $Co_2Mn_xFe_{1-x}Al$ films. The variation in phonon modes with different composition and temperature effects has also been discussed in detail.

2 Experimental details

The $Co_2Mn_xFe_{1-x}Al$ films with a thickness of 30 nm were deposited on GaAs (001) by the molecular-beam epitaxy method at a substrate temperature of 160 °C. The Mn composition x is varied from 0 to 1. All the films were capped with an aluminium

[a]*Key Laboratory of Polar Materials and Devices, Ministry of Education, Department of Electronics Engineering, East China Normal University, Shanghai, 200241, People's Republic of China.*
E-mail: zghu@ee.ecnu.edu.cn; Fax: +86-21-54345119;
Tel: +86-21-54345150
[b]*State Key Laboratory of Superlattice and Microstructures, Institute of Semiconductors, Chinese Academy of Sciences, P.O. Box 912, Beijing, 100083, People's Republic of China*

View Article Online

Published on 16 August 2012. Downloaded on 25/12/2014 07:15:28.

layer of thickness 2 nm to avoid oxidation. The crystal structure and order degree were analyzed by double-crystal X-ray diffraction (DCXRD) and high-resolution transmission electron microscopy (HR-TEM). Temperature-dependent Raman scattering experiments were carried out by a Jobin-Yvon LabRAM HR 800 UV micro-Raman spectrometer, with a 2400 g mm^{-1} grating and an air-cooled charge-coupled device (CCD) detector. The experiments are operated on a Linkam THMSE 600 heating/cooling stage from 87 to 873 K. A He-Cd laser with a wavelength of 325 nm (3.82 eV) was applied as the exciting light. The magnetic properties of the films were obtained by a physical property measurement system (Quantum Design PPMS-9). Note that all the samples were measured at RT and no mathematical smoothing has been performed on the experimental data.

3 Results and discussions

Generally, for full Heusler alloys the crystal structure can be divided into three types: $L2_1$, B_2 and A_2. Among all three types, the $L2_1$ structure (Fig. 1(a)) is the most ordered phase; partial disorder leads to B_2 and full disorder contributes to the A_2 structure. It should be noted that these ordered/disordered structures can be uniquely identified by combining XRD and TEM analysis. This is based on the following relations between atomic ordering and superlattice diffraction lines: the partially disordered B_2 extinguishes the odd superlattice diffraction lines, which are defined by the index relation of h, k, and l = odd numbers, *e.g.*, (111). However, superlattice diffraction lines [$(h + k + l)/2 = 2n + 1$, *e.g.* (200)] vanish under fully disordered A_2.[13] From the DCXRD data, it can be found that the effective cubic lattice constant increases from 5.68 to 5.73 Å as the Mn content increases from 0 to 1. It should be emphasized that the films have almost the same diffraction features despite having different Mn composition.[14] Only the (004) diffraction peak of the $Co_2Mn_xFe_{1-x}Al$ films can be observed besides the (004) and (002) diffractions from the GaAs substrate,[14] indicating a perfect (001)-oriented growth in the direction perpendicular to the film plane. Nevertheless, it has been reported that the (004) reflection is the fundamental characteristic, which cannot be affected by the disorder status.[15] Therefore, one can conclude that all the films are determined to be crystalline in structure, from the present XRD patterns.

We further carried out the HR-TEM measurements to confirm the degree of order for the as-prepared $Co_2Mn_xFe_{1-x}Al$ films. In order to avoid the influence of the aluminium layer, an uncapped

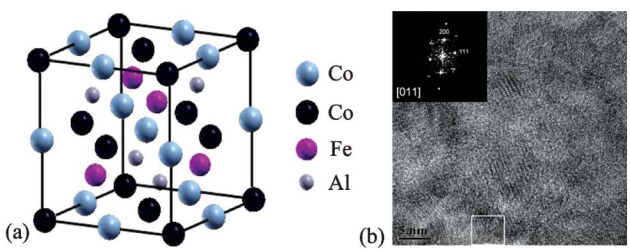

Fig. 1 (a) The crystal structure of $Co_2Mn_xFe_{1-x}Al$ Heusler alloys. (b) Transmission electron micrograph of the Co_2FeAl film. The inset shows fast Fourier transform (FFT) analysis performed on the area squared in the TEM image. Note that the electron beam is parallel to the [110] direction of the Co_2FeAl film.

Co_2FeAl film fabricated by the same method was taken for the HR-TEM experiment. The result is shown in Fig. 1(b) and the inset diffraction pattern shows fast Fourier transform (FFT) analysis of the HR-TEM image, which was performed by Gaten Digital Micrograph software. Both the (111) and (002) diffraction patterns can be clearly observed in the FFT analysis with the electron beam parallel to [110] zone axis of the Co_2FeAl film, in which the (111) diffraction is definitely from the distinct $L2_1$ reflection.[16] Several other HR-TEM images were taken from different positions of the film and fast Fourier-transform (FFT) analyses were also carried out for all of them. The results are similar, which suggests that the films belong to the same structure. It should be emphasized that the films are polycrystalline owing to different orientations of the TEM experiments. Based on the above structure analysis, the present $Co_2Mn_xFe_{1-x}Al$ films can be considered as having the $L2_1$ structure.

$Co_2Mn_xFe_{1-x}Al$ crystallized in the $L2_1$ structure consists of eight stacked body-centered cubic (bcc) lattice. The outer sublattice that consists of the eight cubic lattices is occupied by Co atoms, and the inner cubic sublattice that consists of the body-centered sites of each bcc lattice is regularly occupied by Fe/Mn and Al atoms.[13] It can be seen that the whole crystal presents the tetrahedral T_d symmetry. Meanwhile, each Fe/Mn has eight Co atoms as immediate neighbors, which sit in an octahedral symmetry position. In other words, the lattice consisting of Co atoms has O_h symmetry, where the Co atoms have two different but chemically equivalent positions. The environment of the first sublattice is the same as the environment of the second one but rotated by 90°. The occupancy of two face-centered cubic (fcc) sublattices by the Co atoms separates the full-Heusler alloys with the $L2_1$ structure from the half-Heusler compounds with the $C1_b$ structure, in which only one sublattice is occupied while the other is empty. Note that the $L2_1$ structure, which belongs to space group $Fm\bar{3}m$, represents the most ordered phase of the Co_2-based Heusler compounds.[17]

Heusler alloys are traditionally considered to have outstanding magnetic properties. As an example, Fig. 2 presents the magnetic hysteresis (M–H) curves of Co_2FeAl and $Co_2Mn_{0.3}Fe_{0.7}Al$ measured at RT temperature in the field range −1500 to 1500 Oe. It can be found that both of the films show well-defined ferromagnetic features. The magnetization is normalized to the saturation magnetization M_s. It can be found that the magnetization becomes lower with Mn doping composition. This is ascribed to a larger magnetic moment of the Fe element. Unfortunately, magnetic hysteresis curves of the samples at high temperature cannot be measured because of the limitations of the experimental conditions. Meanwhile, it has been reported that the $Co_2Mn_xFe_{1-x}Al$ films have more complex magnetic phases as x increases to 0.7 and 1.[14] Therefore, one can expect that it is difficult to extract T_c, even by taking high-temperature M–H measurements. Fortunately, the Raman spectrum appears to be an effective method of judgment.

Raman scattering is sensitive to the coordination of local symmetry resulting from atomic substitution and distortion of polyhedra.[18] So it can reveal important information regarding temperature-induced phase transformation. Raman spectra of the $Co_2Mn_xFe_{1-x}Al$ films with x = 1, 0.7, 0.3, and 0 at the low temperature of 87 K are shown in Fig. 3. It should be mentioned

 This journal is © The Royal Society of Chemistry 2012

View Article Online

Published on 16 August 2012. Downloaded on 25/12/2014 07:15:28.

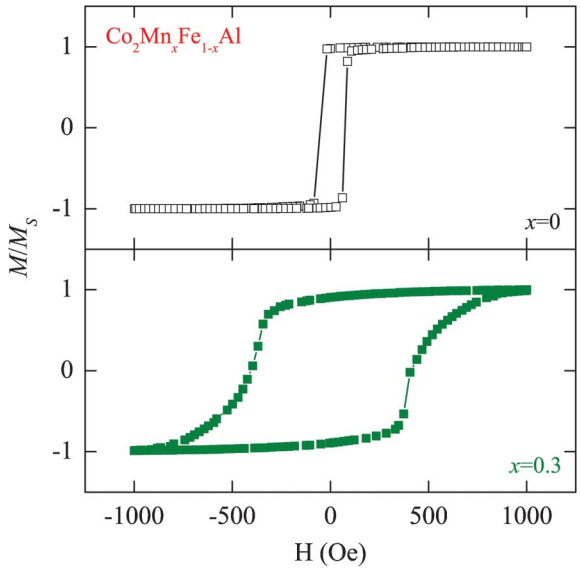

Fig. 2 Room temperature magnetic hysteresis loops (M–H curves) of the $Co_2Mn_xFe_{1-x}Al$ films with $x = 0$ and $x = 0.3$, respectively. Note that the magnetization is normalized to the saturation magnetization M_s.

that the weak scattering intensity could be due partially to the low laser power and experimental configuration, which can offer different signals of the phonon modes.[19] The 2 nm aluminium layer also has some influence on the experimental observations. Three distinct Raman-active modes of the films, which are located at about 320, 569 and 947 cm^{-1}, can be found in the wavenumber range 200 to 1150 cm^{-1}. For the Heusler compounds, the optical modes are split into three well-separated triply degenerate modes: $\Gamma = F_{2g} + 2F_{1u}$. Of all the modes, F_{2g} is Raman-active while the $2F_{1u}$ modes are IR-active.[11] There have been several reports of the appearance of IR-active modes in Raman spectra.[9,20,21] It mainly stems from the local breaking of symmetry and the existence of an inversion center. The idea has been introduced of Co atoms in $Co_2Mn_xFe_{1-x}Al$ having the O_h symmetry, which is very unstable. Moreover, Heusler compounds crystallized in the $L2_1$ structure also exhibit a center of inversion. Therefore, it can be deduced that the two F_{1u} modes

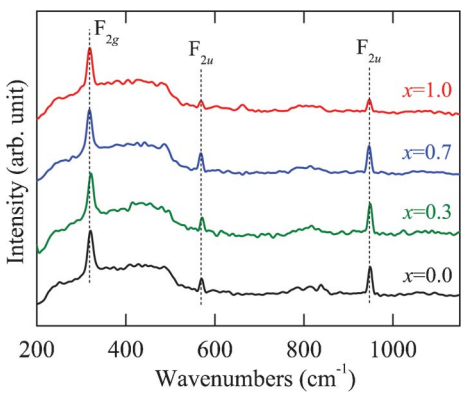

Fig. 3 Raman spectroscopy of the $Co_2Mn_xFe_{1-x}Al$ films with $x = 0$, 0.3, 0.7, and 1 recorded at the temperature of 87 K. The dashed lines show three distinct lattice vibration modes, whose center frequencies present the independence of the Mn composition.

can also be Raman-active in the $Co_2Mn_xFe_{1-x}Al$ films. In conclusion, we attribute these Raman modes to the dominating vibrations of a particular kind of atom.

It is inferred that the vibrational mode at about 320 cm^{-1} corresponds to the F_{2g} phonon. The phonon band can be assigned to the vibrations of the Co atoms in the first sublattice. With regard to the Raman modes located at 569 cm^{-1} and 947 cm^{-1}, they can be attributed to the $2F_{1u}$ phonon modes. These modes involve the vibrations of all atoms together, both the vibrations of the Co atoms in the second sublattice and the impact of the T_d symmetry.[11] It can be seen in Fig. 3 that all the Raman scattering lines have a small full width at half maximum (FWHM). Especially for the phonon modes located at 569 and 947 cm^{-1}, the values of FWHM are within 10 cm^{-1}. It shows that the frequency, band lineshape and relative intensity of the F_{2g} mode at about 320 cm^{-1} are kept constant in the experimental temperature range. This is attributed to the fact that the mode is caused by the vibrations from the Co atoms. As a result, it is independent of the Mn composition. As the Mn composition increases, the frequencies of the $2F_{1u}$ phonon modes remain nearly constant. On the other hand, the intensity shows first an increasing trend and then a slight decline with Mn doping. This could be due to the fact that the atomic mass of Mn is different from that of Fe. When the Mn atoms are introduced, the strength of the lattice vibrations can be affected and leads to differing intensities of the phonon modes. On the other hand, Raman scattering results indicate that the $Co_2Mn_xFe_{1-x}Al$ films are of the $L2_1$ structure, because the B_2 and A_2 types are not Raman-active due to the space groups $Im\bar{3}m$ and $Pm\bar{3}m$, respectively. This agrees well with the previous XRD and TEM results.

In order to further understand the effect of Mn composition on the phase transition behavior in the $Co_2Mn_xFe_{1-x}Al$ films, the temperature dependence of the Raman spectra is presented in Fig. 4 and 5. Although there is no remarkable shift of these phonon modes with increasing temperature, the diverse phonon evolutions of the $Co_2Mn_xFe_{1-x}Al$ films with different Mn compositions can be distinguished. Nevertheless, the frequency

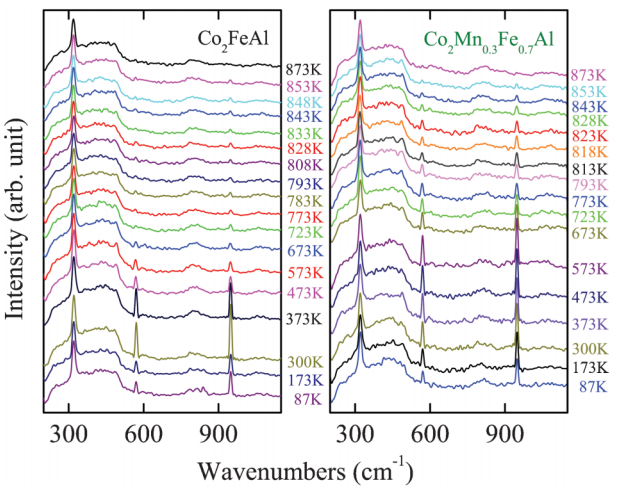

Fig. 4 Raman scattering of the $Co_2Mn_xFe_{1-x}Al$ films with $x = 0$ and $x = 0.3$ at different temperatures. Note that the experimental temperatures selected are different for the films due to the T_c discrepancy.

View Article Online

Published on 16 August 2012. Downloaded on 25/12/2014 07:15:28.

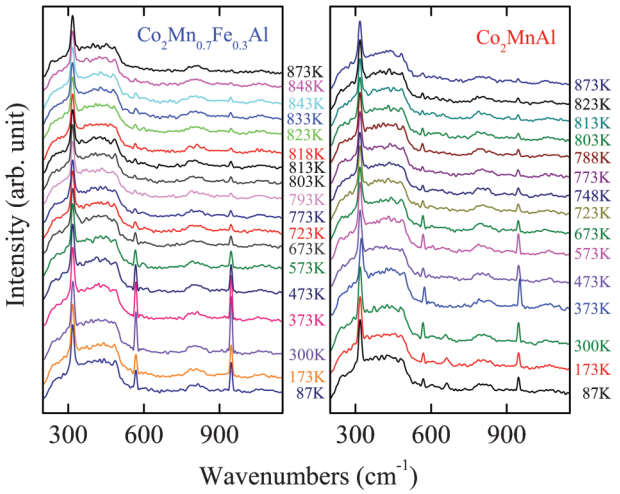

Fig. 5 Raman scattering of the $Co_2Mn_xFe_{1-x}Al$ films with $x = 0.7$ and $x = 1$ in the temperature range 87–873 K. Note that the experimental setting point is different for the two compounds.

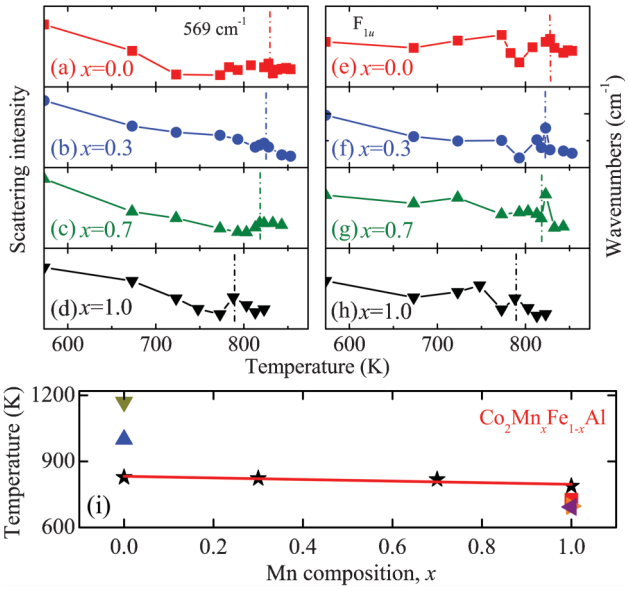

Fig. 6 (a)–(d) The intensity variation of the phonon mode located at 569 cm^{-1} as a function of the temperature for the $Co_2Mn_xFe_{1-x}Al$ films with various Mn compositions. (e)–(h) The frequency variation of the phonon mode located at 947 cm^{-1} as a function of the temperature for the $Co_2Mn_xFe_{1-x}Al$ films. (i) The T_c evolution of the $Co_2Mn_xFe_{1-x}Al$ films with different Mn compositions (★). For comparison, the T_c values are taken from ref. 23 (▲) and ref. 6 (▼) for Co_2FeAl, and ref. 5 (■), ref. 7 (►) and ref. 22 (◄) for Co_2MnAl.

and intensity of the Raman mode at 320 cm^{-1} is qualitatively maintained in the temperature range and no drastic change occurs, which may imply that the vibration of the Co atoms is not sensitive to temperature. The scattering peak of the films detected at 569 cm^{-1} has an obvious increase in intensity until the temperature reaches 300 K and then it begins to decrease gradually and disappears as the temperature approaches 873 K. The frequency of this mode also goes through a complex change. The variation of the frequency and intensity of the Raman mode at 947 cm^{-1} is also similar. This may be because these two phonon modes are associated with both Co atoms and the tetrahedral T_d symmetry. Comparatively, we study the variation in intensity of the mode at 569 cm^{-1} and that of the frequency of 947 cm^{-1}, which are more complex and representative. For all the $Co_2Mn_xFe_{1-x}Al$ films, the peak intensity of the F_{1u} phonon mode at 569 cm^{-1} decreases as the temperature increases above room temperature. However, an abrupt change occurs beyond the phase transition temperature: the intensity of this mode suddenly has a sharp increase with increasing temperature as presented in Fig. 6(a)–(d). The frequency of the Raman mode at 947 cm^{-1} also goes through an abrupt increase with increasing temperature, which is shown in Fig. 6(e)–(h). These phenomena are ascribed to the phase/structural transition in the films. The frequency and intensity increase remarkably and reach a maximum value near but slightly below T_c. Therefore, the phase transition for the $Co_2Mn_xFe_{1-x}Al$ films: 828 K for $x = 0$, 823 K for $x = 0.3$, 818 K for $x = 0.7$, and 788 K for $x = 1$, is represented in Fig. 6(i). It can be confirmed that T_c decreases with increasing Mn composition, which is very consistent with the theoretical results reported.[8]

The variation trend can be expressed by the formula: $T_c(x) = 832 - 36.2x$ $(0 < x < 1)$. It also agrees well with the result of our magnetization measurement, since T_c has a close relationship with the magnetic ordering and a higher moment will contribute to a higher T_c. Note that some other data have been presented for comparison.[5–7,22,23] The T_c values of Co_2MnAl are 726 K,[6] 697 K,[7] and 693 K,[22] while the values of Co_2FeAl are 1170 K[23] and 1000 K.[5] It can be found that the reported values are not in complete agreement with the experimental data in the present work. This may be attributed to different growth methods, which can lead to different surface conditions and quality of the samples. Besides, the difference can be due to the different degrees of atomic long-range ordering of the $L2_1$ structured samples. Different measuring methods and conditions can also induce the discrepancy, such as the heating rate. Note that most of results are taken from theoretical calculations for comparison, because the experimental data are scarcely reported to date. Therefore, one can imagine that the present difference could be acceptable and reasonable. Nevertheless, we can conclude that the present T_c values taken from Raman scattering measurements give a rather good estimation for the $Co_2Mn_xFe_{1-x}Al$ films.

Note that the lattice parameters of Co_2FeAl and Co_2MnAl are $a = 5.68$ Å[24] and 5.73 Å,[25] respectively. Therefore, the lattice constant of $Co_2Mn_xFe_{1-x}Al$ with a higher Mn composition is larger. Exchange energy parameter J is frequently used to calculate different finite-temperature properties, especially for T_c. The relation can be explained by the following equation: $k_B T_c^{MFA} = \frac{2}{3}\sum_i J_{0i}$. Here, k_B is the Boltzmann constant and J_{0i} is the exchange energy between atoms.[7] In the case of more than one magnetic atom per unit cell one has to diagonalize the J_0 matrix of the different sublattice interactions. The T_c can be calculated from the largest eigenvalue J_{max}. Obviously, the T_c is proportional to the exchange energies, which have a close relationship with the lattice parameter. On the other hand, it has been reported that the T_c value determined by the first-principles calculation decreased from 1330 K to 1190 K with decreasing lattice parameter from 0.95 to $1.05a_{exp}$ in Co_2FeGa.[8] And it was also mentioned that there is also the

 This journal is © The Royal Society of Chemistry 2012

View Article Online

Published on 16 August 2012. Downloaded on 25/12/2014 07:15:28.

phenomenon involving Co_2MnAl. It was assigned to a pressure induced T_c enhancement effect because the lattice distortion can be directly related to the pressure factor. It can be inferred that the exchange interaction for $Co_2Mn_xFe_{1-x}Al$ is dominated by the exchange coupling of the Fe–Co/Mn–Co pairs.[26] The variation in interatomic distance for the Fe–Fe/Mn–Mn or Co–Co pairs contributes to the decrease of the Co sublattice's effective exchange coupling constant, while this value of the Fe sublattice increases. As a result, the interplay between the effective exchange coupling constants of the Co and Fe/Mn sublattices results in the pressure induced T_c enhancement of the $Co_2Mn_xFe_{1-x}Al$ films. So we can conclude that the decrease in T_c is due to the fact that the lattice parameter of the $Co_2Mn_xFe_{1-x}Al$ films becomes larger with increasing Mn composition, which is analogous to the results induced by the external pressure.

4 Conclusions

In conclusion, the lattice vibrations of the $Co_2Mn_xFe_{1-x}Al$ films have been studied by temperature-dependent Raman spectroscopy. Three Raman active modes located at about 320, 569 and 947 cm^{-1} can be assigned to the F_{2g} and $2F_{1u}$ modes, respectively. It is found that the latter two modes are sensitive to Mn composition. With the aid of analysis of the lattice vibration of the Raman at 569 and 947 cm^{-1} induced by the structure modification, the T_c point of the $Co_2Mn_xFe_{1-x}Al$ films can be well defined. It shows a linear decrease from 828 to 788 K with the Mn composition, which can be ascribed to the pressure induced T_c enhancement effect.

Acknowledgements

One of the authors (Z. N. Zhan) is grateful to He He, Qing Ren and Prof. Xiaodong Tang for technical support. This work was financially supported by the Natural Science Foundation of China (Grant Nos. 60906046 and 11074076), the Major State Basic Research Development Program of China (Grant No. 2011CB922200), the Projects of Science and Technology Commission of Shanghai Municipality (Grant Nos. 11520701300, 10DJ1400201 and 10SG28), and the Program for Professor of Special Appointment (Eastern Scholar) at Shanghai Institutions of Higher Learning.

References

1 S. Wurmehl, J. Morais, M. d. C. M. Alves, S. R. Teixeira, G. H. Fecher and C. Felser, *J. Alloys Compd.*, 2006, **159**, 423.
2 J. J. Qiu, V. Ko, P. Luo, W. K. Yeo, L. H. An, B. Y. Zong and G. C. Han, *J. Appl. Phys.*, 2009, **105**, 07C932.
3 A. Hütten, J. Schmalhorst, A. Thomas, S. Kämmerer, M. Sacher, D. Ebke, N.-N. Liu, X. Kou and G. Reiss, *J. Alloys Compd.*, 2006, **148**, 423.
4 T. Ambrose, J. J. Krebs and G. A. Prinz, *Appl. Phys. Lett.*, 2000, **76**, 3280.
5 S. Trudel, O. Gaier, J. Hamrle and B. Hillebrands, *J. Phys. D: Appl. Phys.*, 2010, **43**, 193001.
6 R. Y. Umetsu, K. Kobayashi, A. Fujita, R. Kainuma and K. Ishida, *J. Appl. Phys.*, 2008, **103**, 07D718.
7 J. Thoene, S. Chadov, G. Fecher, C. Felser and J. Kübler, *J. Phys. D: Appl. Phys.*, 2009, **42**, 084013.
8 X. B. Liu and Z. Altounian, *J. Appl. Phys.*, 2011, **109**, 07B108.
9 W. J. Zhang, W. W. Li, X. G. Chen, Z. G. Hu, W. Liu, G. S.Wang, X. L. Dong and J. H. Chu, *Appl. Phys. Lett.*, 2011, **99**, 041902.
10 M. J. Han, K. Jiang, J. Z. Zhang, Y.W. Li, Y.W. Li, Z. G. Hu and J. H. Chu, *Appl. Phys. Lett.*, 2011, **99**, 131104.
11 A. T. Zayak, P. Entel, K. M. Rabe, W. A. Adeagbo and M. Acet, *Phys. Rev. B: Condens. Matter Mater. Phys.*, 2005, **72**, 054113.
12 L. Mañosa and A. Planes, *Phys. Rev. B: Condens. Matter*, 2001, **64**, 024305.
13 Y. Takamura, R. Nakane and S. Sugahara, *J. Appl. Phys.*, 2009, **105**, 07B109.
14 K. K. Meng, S. L. Wang, P. F. Xu, L. Chen, W. S. Yan and J. H. Zhao, *Appl. Phys. Lett.*, 2010, **97**, 232506.
15 M. Kogachi, T. Fujiwara and S. Kikuchi, *J. Alloys Compd.*, 2009, **723**, 475.
16 H. Ishikawa, R. Y. Umetsu, K. Kobayashi, A. Fujita, R. Kainuma and K. Ishida, *Acta Mater.*, 2008, **56**, 4789.
17 I. Galanakis and P. H. Dederichs, *Phys. Rev. B: Condens. Matter*, 2002, **66**, 174429.
18 Z. G. Hu, W. W. Li, J. D. Wu, J. Sun, Q. W. Shu, X. X. Zhong, Z. Q. Zhu and J. H. Chu, *Appl. Phys. Lett.*, 2008, **93**, 181910.
19 W. W. Li, J. J. Zhu, J. D. Wu, J. Sun, M. Zhu, Z. G. Hu and J. H. Chu, *ACS Appl. Mater. Interfaces*, 2010, **8**, 2325.
20 O. Okhay, A. Wu, P. M. Vilarinho, I. M. Reaney, A. R. L. Ramos, E. Aleves, J. Petzelt and J. Pokorny, *Acta Mater.*, 2007, **55**, 4947.
21 A. Tkach, T. M. Correia, A. Almeida, J. A. Moreira, M. R. Chaves, O. Okhay, P. M. Vilarinho, I. Gregora and J. Petzelt, *Acta Mater.*, 2007, **59**, 5388.
22 P. J. Webster, *J. Phys. Chem. Solids*, 1971, **32**, 1221.
23 K. Kobayashi, R. Y. Umetsu, R. Kainuma, K. Ishida, T. Oyamada, A. Fujita and K. Fukamichi, *Appl. Phys. Lett.*, 2004, **85**, 4684.
24 B. Balke, G. H. Fecher and C. Felser, *Appl. Phys. Lett.*, 2007, **90**, 172501.
25 J. Kübler, A. R.Williams and C. B. Sommers, *Phys. Rev. B*, 1983, **28**, 1745.
26 H. Kubota, J. Nakata, M. Oogane, Y. Ando, H. Kato, A. Sakuma and T. Miyazaki, *J. Appl. Phys.*, 2005, **97**, 10C913.